Laser Spectroscopy of Cyanoacetylene−Mg_n Complexes in Helium Nanodroplets: Multiple Isomers

F. Dong and R. E. Miller*

Department of Chemistry, University of North Carolina, Chapel Hill, North Carolina 27599

Received: October 28, 2003; In Final Form: January 5, 2004

Infrared laser spectroscopy and ab initio calculations are reported for cyanoacetylene bound to magnesium clusters of varying size, formed and observed in the superfluid helium nanodroplets. Ab initio calculations of the binary HCCCN−Mg potential energy surface reveal three minima. The corresponding isomers are observed experimentally, owing to the unique "growth" conditions provided by liquid helium. The cyanoacetylene is also observed to bind at both the nitrogen and hydrogen ends to larger magnesium clusters in agreement with the minima found in the corresponding ab initio calculations. The infrared spectra show rotational structure that can be fit by the corresponding gas-phase Hamiltonian, using modified constants that account for the effects of the helium solvent. Stark spectroscopy is used to measure the dipole moments of these complexes, providing further insights into the nature of the associated interactions.

Introduction

The field of metal cluster science continues to provide new and fundamental insights into the nature of adsorbate−metal interactions. Studies of this type not only help to bridge our understanding from the molecular to the condensed phase, they also hold the promise of providing a source of new nanomaterials with novel properties.[1−22] This interdisciplinary field spans chemistry, materials science, nanotechnology, and catalysis, making the study of the physical and chemical properties of metal clusters an active area for both experiment and theory.[11,12,19,23−30] Definitive studies now exist that show how significantly the rates and mechanisms of cluster−molecule reactions vary with cluster size,[11,31] suggesting that new nanocatalysts might display novel properties.[31−33]

Despite all that has been learned from these studies, the detailed determination of experimental metal cluster structures is generally lacking. In view of the strong correlation between structure and function, this often makes it difficult to obtain conclusive information on the association chemical mechanisms from such studies. Indeed, the lack of experimental methods for probing structures in metal cluster science has been the subject of much discussion in the literature.[12] Although spectroscopic methods can provide quantitative structural information from rotational constants, only small systems (single metal atom complexes)[34] have been studied in this way. In contrast, chemical probe techniques have been used on much larger systems,[35−38] but usually provide only qualitative information on the binding sites of adsorbates on larger metal clusters.[39] In general, experiments on the chemistry of metal clusters often depend heavily upon ab initio calculations for structural information.

Recent developments in the use of infrared spectroscopy in the helium nanodroplets[40,41−44] have provided methods for determining the structures of metal cluster−adsorbate systems.[45] These experiments often provide rotational resolution even for systems containing multiple metal atoms, while the associated vibrational frequency shifts from the free molecule provide information on the interactions with the metal cluster. Our first application of this approach was on HCN−Mg_n complexes,[45−47] where the experimental results provided compelling evidence for nitrogen-bonded structures. In the case of the binary HCN−Mg complex, two isomers were observed, corresponding to the Mg atom binding to the hydrogen end (H-bonded) and nitrogen end (N-bonded) of the HCN.[46]

In the present study we consider a somewhat more complicated system, namely that of cyanoacetylene bound to Mg_n. Ab initio calculations are also reported here, yielding an HCCCN−Mg potential energy surface (PES) that is quite anisotropic, with three binding sites for the magnesium atom. The corresponding isomers are observed in the helium droplet experiments reported here, as well as those for the clusters with $n > 1$, including both N-bonded and H-bonded complexes for each size. Dipole moments and vibrational frequency shifts are reported for all of these complexes, providing insights into the nature of the corresponding interactions. Comparisons with the corresponding results for hydrogen-bonded complexes (such as $(HCCCN)_n$[48]) reveal that the interactions in HCCCN−Mg_n are highly nonadditive.

Experimental Method

The helium droplet apparatus used in the present study has been described in detail elsewhere.[49] Helium nanodroplets are formed by expanding ultrahigh purity helium (99.9999%) into vacuum through a 5 μm diameter nozzle, maintained at approximately 23 K by a closed cycle helium refrigerator. At a source pressure of 60 atm, the mean droplet size is approximately 4000 helium atoms. The atoms and molecules of interest are added to the droplets via the pick-up process.[50] In particular, the magnesium atoms were captured by the droplets first, as they passed through a metal oven, the temperature of which was used to vary the vapor pressure of the magnesium. The cyanoacetylene was introduced into the droplets by a second pickup cell positioned downstream of the metal oven. The flight time of the droplets between the two pick-up cells is sufficiently long to ensure that the metal atoms have formed a cluster and cooled to the droplet temperature (0.37 K),[41] before the arrival of the cyanoacetylene molecule.

10.1021/jp031194i CCC: $27.50
Published on Web 02/28/2004

The seeded droplets pass through the laser excitation region, where the C−H stretch of the cyanoacetylene is excited by an F-center laser, pumped by a krypton ion laser. Subsequent vibrational relaxation results in the evaporation of approximately 600 helium atoms from the droplet. The corresponding depletion in the helium flux is detected by a bolometer.[51] The spectra are made background free by amplitude modulating the laser, while using phase-sensitive detection methods. A multiple reflection cell was used to reflect the laser through the helium droplet beam many times, greatly improving the excitation probability.

Two electrodes were positioned normal to the multipass cell in order to apply a large DC-electric field to the laser excitation region. In this way, the Stark spectrum[52] of the complex could be measured, from which the permanent electric dipole moment was obtained.[53] At high fields, a significant increase in the signal levels was obtained, as the rotational contour in the vibrational spectrum collapses into a single pendular peak.[45] By recording the dependence of the signal levels for the various vibrational bands on the cyanoactylene and magnesium pressures, firm assignments of the cluster sizes (*m*,*n*) were obtained, *m* and *n* being the numbers of HCCCN molecules and magnesium atoms, respectively. In the present study, the focus is on clusters containing a single HCCCN molecule.

Ab Initio Results for HCCCN−Mg$_n$. The ab initio calculations reported here were performed by using second-order Møller−Plesset perturbation theory (MP2) and the 6-311++G-(3df,3pd) basis set. The associated potential energy surface (PES) was calculated with the Molpro-2000 package,[54] and basis-set superposition error (BSSE) was taken into account by using the counterpoise correction method.[55] The fully optimized geometries for all of the isomers and transition states were calculated with Gaussian98,[56] along with the corresponding vibrational frequencies.

The PES for the binary complex was calculated by freezing the cyanoacetylene monomer at its equilibrium geometry (determined from a separate geometry optimization of the monomer at the same level of theory). A total of 144 points were calculated on the 2-D intermolecular potential, defined by the intermolecular distance and the angle between the Mg atom and the HCCCN molecule, as shown in Figure 1a. Three minima are evident on this PES, the global one ($D_e = 303$ cm^{-1}) corresponding to the magnesium atom binding to the nitrogen end of the molecule (hereafter referred to as the N-bonded isomer). This minimum actually corresponds to a bent geometry (structure **1(a)** in Figure 1b), with the magnesium being ∼35° from the molecular axis and 4.93 Å from the center of mass (COM) of cyanoacetylene. It is interesting to note that the barrier at the linear geometry is quite high (approximately 35 cm^{-1}), compared to that for HCN−Mg (<5 cm^{-1}).[46] In the latter case, we found that the spectrum was indistinguishable from that of a linear molecule, suggesting that the barrier is low enough to make the vibrationally averaged structure effectively linear. The higher barrier evident in the ab initio PES of HCCCN−Mg suggests that this may not be the case for this system. This point will be discussed further in the next section.

A second minimum on the PES ($D_e = 210$ cm^{-1}) is observed at the hydrogen end of the molecule (structure **1(c)** in Figure 1(b), hereafter called the H-bonded isomer), corresponding to a linear structure. The third minimum on the PES ($D_e = 299$ cm^{-1}) corresponds to the magnesium atom being nearly perpendicular to the molecular axis (∼85°) (structure **1(b)** in Figure 1(b)). This structure corresponds rather well to the T-shaped geometry we have recently identified for the acetylene−Mg complex,[57] corresponding to the magnesium atom attached to the acetylenic triple bond.

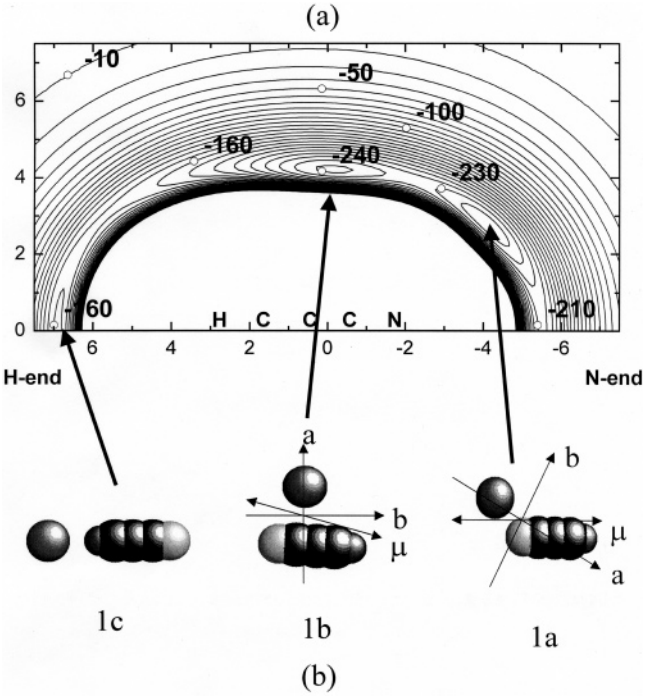

Figure 1. (a) The ab initio potential energy surface (PES) of HCCCN−Mg in Cartesian coordinates, calculated at MP2/6-311++G(3df,3pd) level of theory. The energies were corrected for basis set superposition error (BSSE) by using the counterpoise correction method. The separation between the adjacent contours is 5 cm^{-1}. (b) The structures **1(a)**, **1(b)**, and **1(c)** correspond to the indicated minima on the PES and were obtained from full geometry optimizations.

TABLE 1: Spectroscopic Parameters of Different Isomers of Mg−HCCCN: Comparisons between Experimental Results and ab Initio Calculations at the MP2/6-311++G(3df,3pd) Level

	experimental			MP2/6-311++G(3df,3pd)		
	1a	**1b**	**1c**	**1a**[b]	**1b**[b]	**1c**[b]
ν/cm^{-1}	3326.339	3326.188	3305.32	3325.78[a]	3325.43[a]	3305.99[a]
μ/D			4.5 ± 0.5	4.25	3.55	4.42
A/cm^{-1}	0.197	0.050	- -	0.5360	0.1530	
B/cm^{-1}	0.012	0.020	0.005	0.0353	0.0600	0.0206
C/cm^{-1}	0.011	0.015	0.005	0.0331	0.0431	0.0206
$\Delta\nu$/cm^{-1}	0.651	0.902	21.77	1.31	1.66	21.10
D_e/cm^{-1}				303	299	210
D_0/cm^{-1} [c]				136	139	43

[a] Ab initio frequencies scaled ($f = 0.959$, which is determined from HCCCN monomer calculation at the same level). [b] Structures are shown in Figure 1. [c] Dissociation energy after harmonic zero-point energy corrected.

Geometry optimizations were carried out for all three of the minima discussed above, the results of which are summarized in Table 1. For all three cases there were no imaginary frequencies, consistent with these being real minima on the PES. The ab initio frequency shifts for the C−H stretching vibrations of these three isomers are given in Table 1. These were obtained by first scaling the vibrational frequencies of the complex and the monomer by 0.959, namely that needed to bring the harmonic C−H stretching frequency of the cyanoacetylene monomer into agreement with the experimental value. By using harmonic zero-point energies (ZPE), the D_0 binding energies were determined to be 136, 139, and 43 cm^{-1} for structures **1(a)**, **1(b)**, and **1(c)**, respectively.

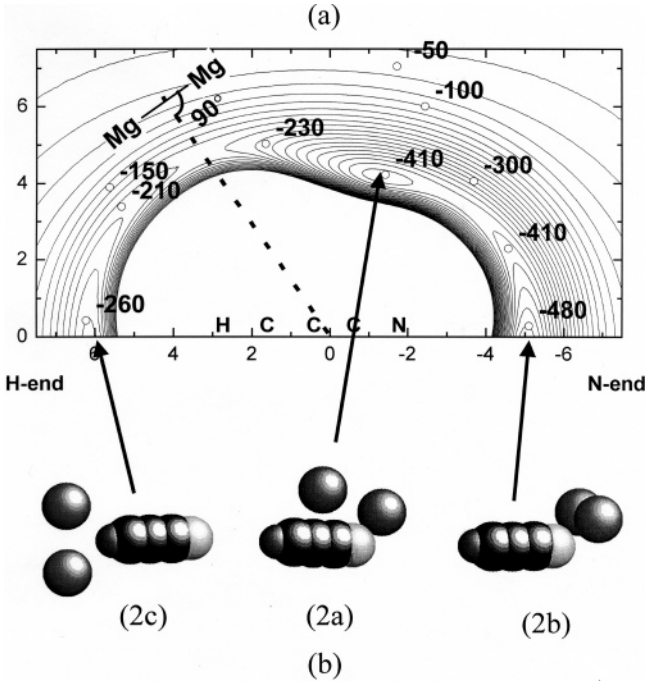

Figure 2. (a) A cut though the PES of HCCCN−Mg_2 in Cartesian coordinates, calculated at MP2/6-311++G(3df,3pd) level of theory. The distance between two magnesium atoms was held fixed at 3.89 Å, and the angle between the line joining the centers of mass of the molecule and the magnesium dimer and the axis of the latter was held fixed at 90°, as shown in the inset. The energies were corrected for BSSE by using the counterpoise correction method. The separation between the adjacent contours is 10 cm^{-1}. (b) A scan of the four-dimensional PES and ab initio geometry optimizations revealed the three geometries labeled as **2(a)**, **2(b)**, amd **2(c)**.

Previous studies from our group have shown that cluster growth in helium droplets often results in the formation of higher energy isomers,[58] particularly when the barriers between the corresponding minima on the PES are moderately large, so that at the low temperature of the droplets there is no interconversion. The ab initio barriers were determined by searching for the transition states between the three isomers, yielding ∼18 cm^{-1} for the barrier between the two bent geometries (**1(a)** and **1(b)**) and ∼10 cm^{-1} between structures **1(b)** and **1(c)**, including the harmonic ZPE correction. As shown below, all three of these isomers are observed in the present helium droplet experiments, indicating that these barriers are sufficiently high to prevent the isomers from interconverting.

Ab initio calculations were also performed for complexes containing multiple magnesium atoms. Since the magnesium atoms were added to the helium droplet prior to the molecule, we only considered structures where the magnesium atoms form a compact cluster. In other words, we have not considered clusters in which the magnesium atoms are separated from one another in widely spaced mimima on the PES. In fact, we have observed such species, by changing the pick-up sequence, although the discussion of these is beyond the scope of the present paper.

It is interesting to note that the distance between minima **1-(a)** and **1(b)** on the PES discussed above is nearly identical with the bond length of the magnesium dimer. This suggests that one of the stable isomers of HCCCN−Mg_2 will have the two magnesium atoms accommodated in these minima, giving rise to the planar structure **2(a)** shown in Figure 2b (D_e = 684 cm^{-1}). Another possibility is a "T-shaped" cluster, having the magnesium dimer bound to the nitrogen end of the cyanoacetylene. In this case, the Mg_2 bond length is much shorter than the diameter of the trough in the PES of the binary complex (∼5.72 Å) going around the molecular axis (at the nitrogen end of the molecule) so we might expect that the corresponding structure will be somewhat nonplanar (structure **2(b)** in Figure 2(b)) (D_e = 708 cm^{-1}). Finally, the magnesium dimer can be placed at the hydrogen end of the molecule, giving rise to a "T-shaped" structure (structure **2(c)** in Figure 2b) (D_e = 317 cm^{-1}). In this case, the corresponding minimum in the PES of the binary complex is in the linear geometry so that the equilibrium geometry of this T-shaped complex is planar. The latter is much more weakly bound than the other two, simply based on the depths of the wells on the PES of the binary complex.

TABLE 2: Spectroscopic Parameters of Different Isomers of Mg_2−HCCCN: Comparisons between Experimental Results and ab Initio Calculations at the MP2/6-311++G(3df,3pd) Level

	experimental			MP2/6-311++G(3df,3pd)		
	2a	**2b**	**2c**	**2a**[b]	**2b**[b]	**2c**[b]
ν/cm^{-1}	3325.302	3325.389	3297.60	3324.37[a]	3324.57[a]	3298.81[a]
μ/D			4.8 ± 0.5	3.92	4.52	4.89
A/cm^{-1}	0.018	0.036	0.020	0.0732	0.0855	0.0815
B/cm^{-1}	0.011	0.013	0.0055	0.0315	0.0235	0.0172
C/cm^{-1}	0.009	0.010	0.0045	0.0220	0.0184	0.0142
$\Delta\nu$/cm^{-1}	1.694	1.606	29.49	2.72	2.52	28.28
D_e/cm^{-1}				684	708	317
D_0/cm^{-1} [c]				483	516	119

[a] Ab initio frequencies scaled (f = 0.959, which is determined from HCCCN monomer calculation at the same level). [b] Structures are shown in Figure 2. [c] Dissociation energy after harmonic zero-point energy corrected.

The four-dimensional intermolecular PES for the HCCCN−Mg_2 was scanned with Gaussian98 (magnesium dimer distance fixed at 3.89 Å), searching for different isomers. These calculations revealed only the minima suggested above. These are illustrated in the planar 2-D slice through the potential shown in Figure 2a, where the angle between the line joining the centers of mass of the Mg_2 and the cyanoacetylene and the Mg_2 bond axis is also fixed at 90°. Although the minimum at the nitrogen end of the cyanoactylene is actually nonplanar, it is already evident in this planar slice. It is interesting to note that the barriers between these minima are larger than those on the PES of the binary complex, namely ∼70 cm^{-1} between **2(a)** and **2(c)** and ∼120 cm^{-1} between **2(a)** and **2(b)**.

Geometry optimizations were carried out for all three HCCCN−Mg_2 isomers and the results are summarized in Table 2. The optimized geometries (Figure 2b) are in good agreement with the above arguments, based on the PES of the binary complex. The corresponding D_0 binding energies obtained after applying the harmonic zero-point energy corrections are 483, 516, and 119 cm^{-1} for isomers **2(a)**, **2(b)**, and **2(c)**, respectively.

A cut through the ab initio HCCCN−Mg_3 PES is shown in Figure 3a (constructed from 180 points). In this case the line joining the centers of mass of cyanoacetylene and the magnesium trimer is maintained perpendicular to the trimer plane and the bond lengths of Mg_3 are fixed at 3.31 Å (as shown in the inset). In this case we see only two minima, namely a deep well (D_e = 1795 cm^{-1}) at the nitrogen end of the molecule (structure **3(a)**) and a relatively shallow well (D_e = 671 cm^{-1}) at the hydrogen end (structure **3(b)**). The barrier between these two minima is less than 10 cm^{-1}. The barrier is not evident in the PES shown in Figure 3 simply due to the course spacing between the contours, illustrating that the calculated barrier is very small. Full geometry optimizations confirm the existence

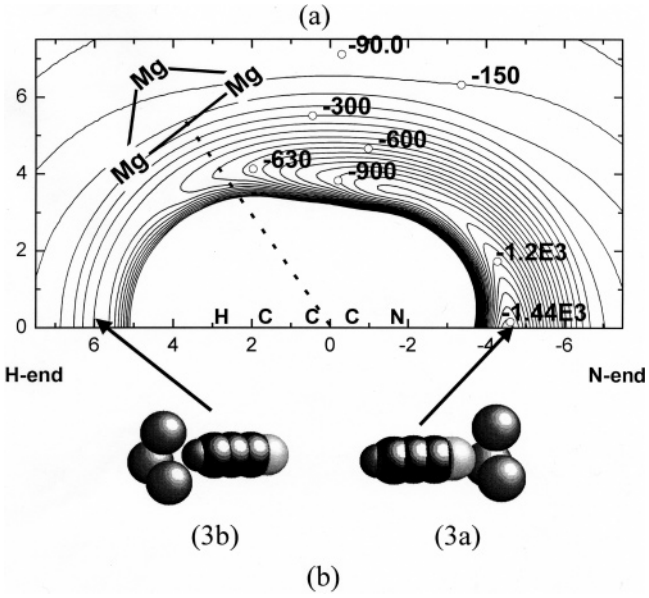

Figure 3. (a) The PES of HCCCN−Mg_3 in Cartesian coordinates, with the configuration shown as an inset, calculated at MP2/6-311++G-(3df,3pd) level with BSSE corrections. The distances between the magnesium atoms were fixed at 3.31 Å. The plane of the equilateral triangle of Mg_3 was set to be normal to the line connecting the center of mass of Mg_3 and HCCCN molecules. The separation between the adjacent contours is 60 cm^{-1}. (b) The two optimized geometries, **3(a)** and **3(b)**, both have C_{3v} symmetry, corresponding to the minima indicated by the arrows.

TABLE 3: Spectroscopic Parameters of Different Isomers of Mg_3−HCCCN: Comparisons between Experimental Results and ab Initio Calculations at the MP2/6-311++G(3df,3pd) Level

	experimental		MP2/6-311++G(3df,3pd)	
	3a	**3b**	**3a**[b]	**3b**[b]
ν/cm^{-1}	3323.673	3282.15	3321.41[a]	3287.32[a]
μ/D	5.0 ± 0.2	4.9 ± 0.4	5.08	4.74
A/cm^{-1}	0.028	0.025	0.0683	0.0616
B/cm^{-1}	0.0065	0.0045	0.0210	0.0143
C/cm^{-1}	0.0065	0.0045	0.0210	0.0143
$\Delta\nu$/cm^{-1}	3.417	44.94	5.68	39.77
D_e/cm^{-1}			1795	671
D_0/cm^{-1} [c]			1520	530

[a] Ab initio frequencies scaled ($f = 0.959$, which is determined from HCCCN monomer calculation at the same level). [b] Structures are shown in Figure 3. [c] Dissociation energy after harmonic zero-point energy corrected.

of two minima corresponding to the N-bonded and H-bonded isomers. Both of these are C_{3v} symmetric top structures (structure **3(a)** and **3(b)** in Figure 3b, respectively). Table 3 summarizes the ab initio calculations for both isomers. The interaction energies for structures **3(a)** and **3(b)** are −1520 and −530 cm^{-1}, respectively, after harmonic zero-point energy corrections.

The global minimum on the Mg_4 PES is well-known to correspond to the tetrahedral structure.[2,59,60] In studies of HCN−Mg_4 carried out in our laboratory, we identified a complex in which the nitrogen of HCN binds to a single magnesium atom of Mg_4 (on-top structure), resulting in a complex with C_{3v} symmetry. Ab initio calculations confirmed that this is the most stable isomer for this system.[47] Analogous calculations for HCCCN−Mg_4 reveal that the same on-top structure is the most strongly bonded isomer (structure **4(a)** in Figure 4) ($D_e = 2239$ cm^{-1}). However, in this case a full geometry optimization yields a structure in which the molecule is slightly tilted off the C_{3v} axis, as shown in Figure 4. A second isomer is predicted by the ab initio calculations, corresponding to the hydrogen end of the HCCCN pointing toward the magnesium cluster, in these cases on one of the faces of the tetrahedral (see structure **4(b)** in Figure 4) ($D_e = 946$ cm^{-1}), which in surface science would be called a 3-fold binding site. The results from the optimized structures for these two isomers are summarized in Table 4. The binding energies after zero-point energy corrections for structures **4(a)** and **4(b)** are 1891 and 820 cm^{-1}, respectively.

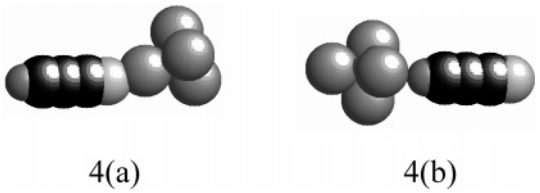

Figure 4. Ab initio optimized structures for HCCCN−Mg_4, corresponding to the nitrogen bonded, on-top geometry **4(a)** and hydrogen bonded, 3-fold structure **4(b)**. The optimized structure for **4(a)** is somewhat tilted, while the hydrogen-bonded complex has C_{3v} symmetry.

TABLE 4: Spectroscopic Parameters of Different Isomers of Mg_4−HCCCN: Comparisons between Experimental Results and ab Initio Calculations at the MP2/6-311++G(3df,3pd) Level

	experimental		MP2/6-311++G(3df,3pd)	
	4a	**4b**	**4a**[b]	**4b**[b]
ν/cm^{-1}	3318.685	3263.20	3318.68[a]	3261.54[a]
μ/D	9.6 ± 0.4	5.0 ± 0.4	9.99	5.09
A/cm^{-1}	0.035	0.035	0.077	0.076
B/cm^{-1}	0.0050	0.0044	0.011	0.0092
C/cm^{-1}	0.0050	0.0044	0.011	0.0092
$\Delta\nu$/cm^{-1}	8.405	63.89	8.45	65.55
D_e/cm^{-1}			2239	946
D_0/cm^{-1} [c]			1891	820

[a] Ab initio frequencies scaled by $f = 0.962$. [b] Structures are shown in Figure 4. [c] Dissociation energy after harmonic zero-point energy corrected.

The ab initio vibrational frequency calculations for all of these complexes indicate that the associated C−H stretches are all shifted to the red, relative to the HCCCN monomer. As expected, the calculated shifts for the N-bonded complexes are small relative to those of the H-bonded isomers (see Tables 1−4). For the N-bonded complexes, the red shift increases rather smoothly with increasing metal cluster size, from Mg−HCCCN to Mg_3−HCCCN, with a sudden increase for HCCCN−Mg_4. The calculated dipole moments of the smaller systems ($n = 1-3$) are generally incrementally larger than that of the monomer, consistent with the induced dipole on the magnesium cluster. The one exception is the N-bonded on-top isomer of HCCCN−Mg_4, for which the dipole moment is qualitatively larger (9.9 D), suggestive of charge transfer between the molecule and the Mg_4 complex. This will be discussed further in later sections of this paper.

Experimental Results

We have shown in a number of previous studies that the sensitivity of helium droplet spectroscopy can be improved considerably by using the pendular state method.[45] As a result, initial searches for the magnesium−cyanoacetylene clusters were carried out with a large electric field (~50 kV/cm) applied to the laser-droplet interaction region. Using the HCN−Mg_n results as a guide[46,47] (since the experiments were performed before

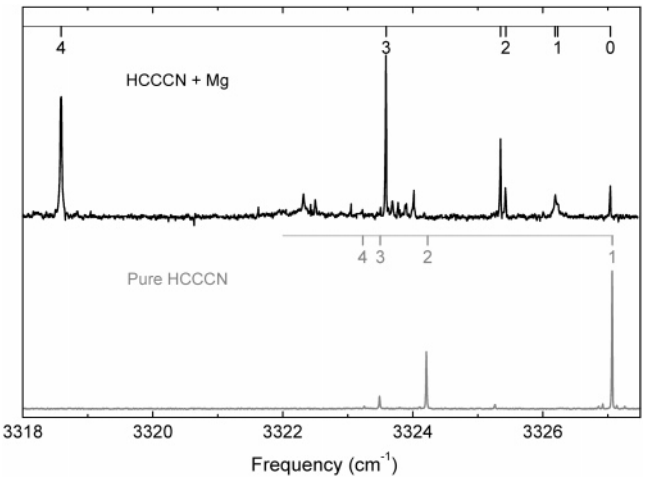

Figure 5. Infrared pendular spectra of the free C−H stretches for (bottom panel) pure $(HCCCN)_m$ ($m = 1-4$) complexes and (top panel) HCCCN−Mg_n ($n = 1-4$) N-bonded complexes.

the ab initio calculations), we expected that the C−H stretch of HCCCN in the nitrogen-bonded complexes would only be weakly shifted from the cyanoacetylene monomer. Figure 5 shows a comparison between two pendular spectra, the top panel having been recorded under conditions that optimize for the formation of HCCCN−Mg_n complexes, while in the lower panel the magnesium oven was switched off so that the helium droplets only contain cyanoacetylene. The spectra of the linear cyanoacetylene clusters (lower panel) formed in the helium droplets have been discussed previously[48] and are labeled in the figure. The new peaks that appear when the magnesium oven is heated can be assigned to the HCCCN−Mg_n complexes, with the size determined from the way in which the intensities of the various bands vary with magnesium pressure in the oven.

The latter point is illustrated in Figure 6b, which shows a series of pendular spectra recorded as a function of the magnesium oven temperature. The broad feature (1,1) in the figure (1 cyanoacetylene and 1 magnesium atom, respectively) was the first to appear at low oven temperatures and disappeared quickly at higher temperatures. The fact that the shape of the band does not change with oven temperature suggests that all of the corresponding signal comes from (1,1) complexes. This assignment is also consistent with the fact that the band is the least shifted from the monomer. Note that the peak labeled (2,0) (cyanoacetylene dimer) simply decreases with increasing oven temperature, as is the case for the monomer (1,0) (not shown).

Figure 6a shows the (cyanoacetylene) pick-up cell pressure dependence of several of the bands in the spectrum. The fact that all of these Poisson distributions peak at the same pick-up cell pressure confirms that they are all associated with complexes that contain only a single cyanoacetylene monomer. The combination of the metal oven temperature dependence and the cyanoacetylene pick-up cell pressure dependence provides unambiguous assignments of the cluster compositions (m,n). Several bands are also identified in the spectra that are clearly due to complexes containing more than one cyanoacetylene molecule, although the discussion of these is beyond the scope of the present work.

HCCCN−Mg_1. As noted above, the pendular spectrum of the (1,1) complex in Figure 6b is quite broad relative to the others in the spectrum. This is further illustrated in the expanded view of this spectrum, shown in Figure 7a, along with a scan of the same spectral region recorded in the absence of an electric field. Analogous spectra obtained for the HCN−Mg complex

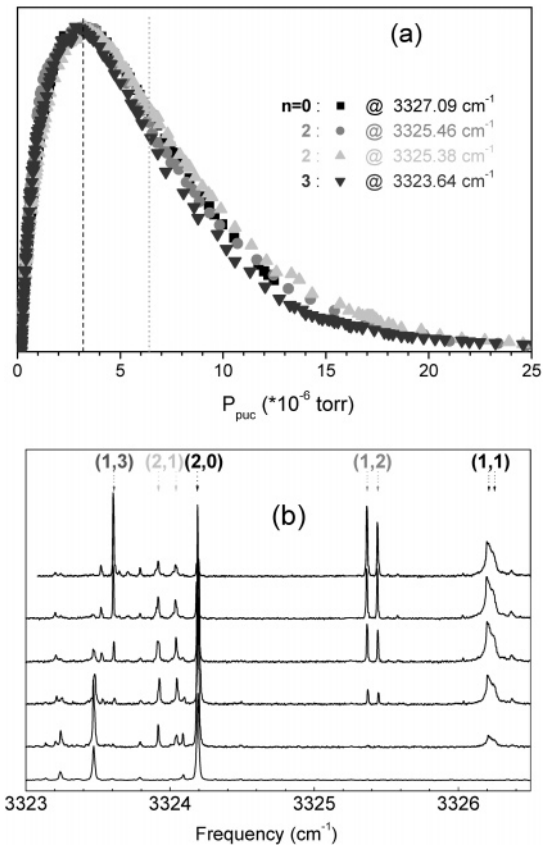

Figure 6. (a) The dependence of the intensity of the pendular spectra of HCCCN−Mg_n complexes on the HCCCN pick-up cell pressure. The dashed and dotted lines are the pressures that optimize for the pick-up of one or two HCCCN molecules, respectively. (b) A series of pendular spectra recorded as a function of the magnesium oven temperature, used to assign the bands to different cluster sizes. The transitions are labeled as (m,n), where m is the number of HCCCN molecules in the cluster and n is the number of magnesium atoms.

showed well-resolved rotational fine structure, providing information on the molecular symmetry and rotational constants, which were qualitatively compared with the ab initio calculations (after applying a simple factor of 3 correction to account for the effects of the helium[40]). Unfortunately, the zero-field spectrum shown here is not fully resolved, which makes sense given that the candidate complexes (shown in Figure 1) are asymmetric tops and the cyanoacetylene is considerably heavier than HCN. In the absence of theoretical guidance, a unique assignment of this spectrum would be difficult, particularly given that we were unable to fit the zero-field spectrum to a single ro-vibrational band. This is consistent with the fact that isomers **1(a)** and **1(b)** have similar ab initio C−H stretch frequency shifts (from the monomer), namely 1.31 and 1.66 cm^{-1}, respectively. As a result, we expect the spectra of these two isomers to overlap.

Combined with the fact that the spectra associated with these two isomers are both hybrid bands, this could also account for the broadening observed in the pendular spectrum. Using the ab initio structures as a guide (starting rotational constants and relative contributions from A-type and B-type bands), we obtained a reasonable fit to the zero-field spectrum, shown in Figure 7a. The constants used to generate these calculated spectra are summarized in Table 1. The fitted rotational constants are reasonable, namely a factor of ∼3 smaller than the ab initio values, owing to the effects of the helium.[40] In addition, the difference in the fitted vibrational band origins for these two bands is consistent with the ab initio calculations

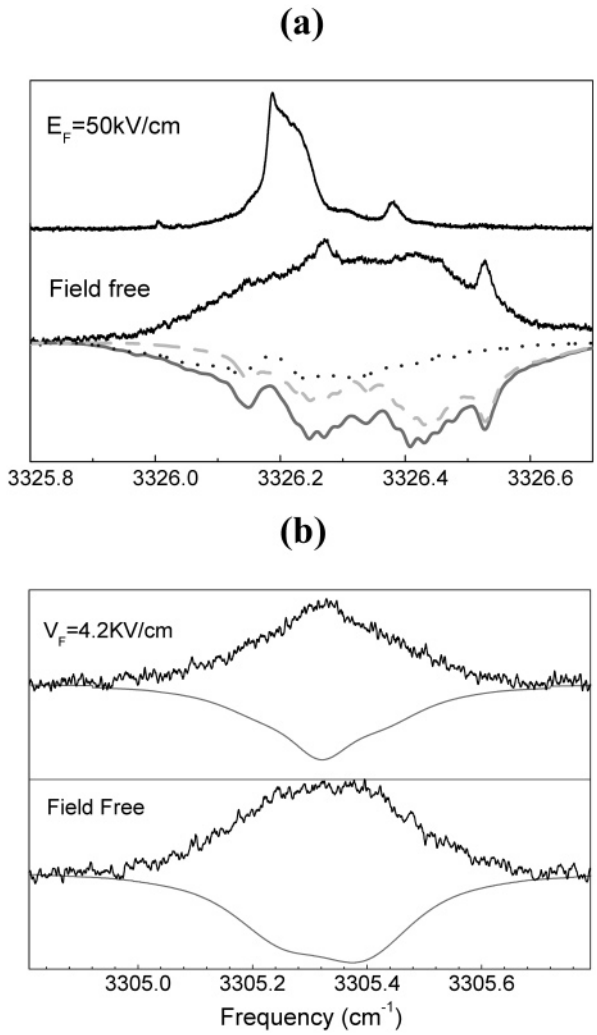

Figure 7. Field free and pendular spectra for HCCCN−Mg, corresponding to the N-bonded (a) and H-bonded (b) isomers. The spectra in panel (a) correspond to the overlap of the two N-bonded isomers, namely **1(a)** and **1(b)** in Figure 1. The fit to the overall field free rotational contour consists of the sum of two spectra, generated assuming the ab initio structures and rotational constants that are modified to approximately account for the effects of the helium. The spectra of H-bonded isomers (b) are consistent with a linear molecule (structure **1(c)** in Figure 1). The dipole moment, obtained by fitting the Stark spectrum, is approximately 4.5 D.

for isomers **1(a)** and **1(b)** and the results from the pendular spectrum. The most we can say from this analysis is that the experimental spectra are consistent with both of these isomers being formed in the helium droplets. As we will see in what follows, the correspondence between the experimental and theoretical data is excellent for the larger cluster sizes, giving us considerable confidence in the above assignment.

As indicated in Table 1, ab initio calculations suggest that the linear H-bonded isomer of the binary complex has a much larger frequency shift (∼21.1 cm^{-1}) than the two considered above, owing to the close proximity of the magnesium to the C−H. Searches were carried out in this spectral region, resulting in the observation of the band shown in Figure 7b. Here again, the spectrum is not fully rotationally resolved, although it does show a clear P/R contour that is consistent with a linear molecule. It is interesting to note that even in the lighter Mg−HCN complex,[46] the hydrogen-bonded isomer showed a similarly broad spectrum, presumably due to fast vibrational relaxation resulting from the strong coupling between the intermolecular degrees of freedom and the C−H stretching vibration, due to the close proximity of the magnesium to the latter.

The smooth line in Figure 7b is a fit to a linear molecule Hamiltonian, with the corresponding rotational constants summarized in Table 1. It is important to note that the spacing between the P and R branches provides a reasonable measure of the rotational constants of this species, because we know the rotational temperature, characteristic of the droplets. The ratio of the ab initio and experimental rotational constants for this species is approximately 2.5, quite reasonable for a molecule in helium. Note that the ab initio (21.1 cm^{-1}) and experimental (21.77 cm^{-1}) frequency shifts are in excellent agreement and that the oven temperature and cyanoacetylene pick-up cell pressure dependence of this band confirm that it is a (1,1) complex. Pendular spectroscopy was also used to estimate the dipole moment of this complex (∼4.5 D), which is also in excellent agreement with the ab initio value (4.42 D). Note that the dipole moment of the cyanoacetylene monomer is 3.72 D.[61] The combination of all of these results provides a firm assignment of this spectrum to the most weakly bound isomer of the binary complex, namely **1(c)** in Figure 1b.

HCCCN−Mg_2. In the pendular spectra shown in Figure 6b there are two bands assigned to (1,2) complexes based upon the oven temperature and pick-up cell pressure dependence of the associated signals. Here again, we see that the relative intensities of these two bands do not depend on the oven temperature and pick-up cell pressure, indicating they have the same composition. Note that these peaks grow in more slowly than those assigned as (1,1) complexes, consistent with the fact that their formation requires the pick-up of two magnesium atoms, and thus higher oven temperatures. The experimental vibrational frequency shifts are in quite good agreement with the ab initio calculations for isomers **2(a)** and **2(b)** (see Figure 2b), as shown in Table 2. It is also interesting to note that the frequency shifts for these isomers are somewhat less than double that of the (1,1) complexes, consistent with the fact that two magnesium atoms cannot interact quite as efficiently with the molecule as they can independently, due simply to steric effects. A similar effect was seen for HCN−Mg_2[45] and is also typical of complexes containing multiple rare gas atoms.[62] All indications are that the magnesium dimer is a van der Waals complex, making this additive description of the associated interactions quite reasonable.

Given that the vibrational origins for these two bands are accurately determined from the pendular spectrum, the fitting of the zero-field spectrum is more straightforward than that for the Mg−HCCCN systems discussed above. Here again, however, the spectrum is not fully resolved, because these complexes are asymmetric tops with quite complex spectra. Figure 8a shows a comparison between the pendular and field free spectra for HCCCN−Mg_2 complexes, along with a fit to the zero field spectrum, obtained with some guidance from the ab initio calculations, as discussed below. In these spectra, the well-defined Q branches in the field free spectrum line up rather well with the pendular transitions, confirming that the latter provide an accurate measure of the corresponding vibrational origins. The P and R branches are rather well resolved in this spectrum, aiding in the fitting of the spectrum. The smooth lines in the figure show the fitted zero-field spectrum, which is in excellent agreement with the experiment. Note that we once again find that the fitted rotational constants are approximately a factor of 3 smaller than the ab initio values.

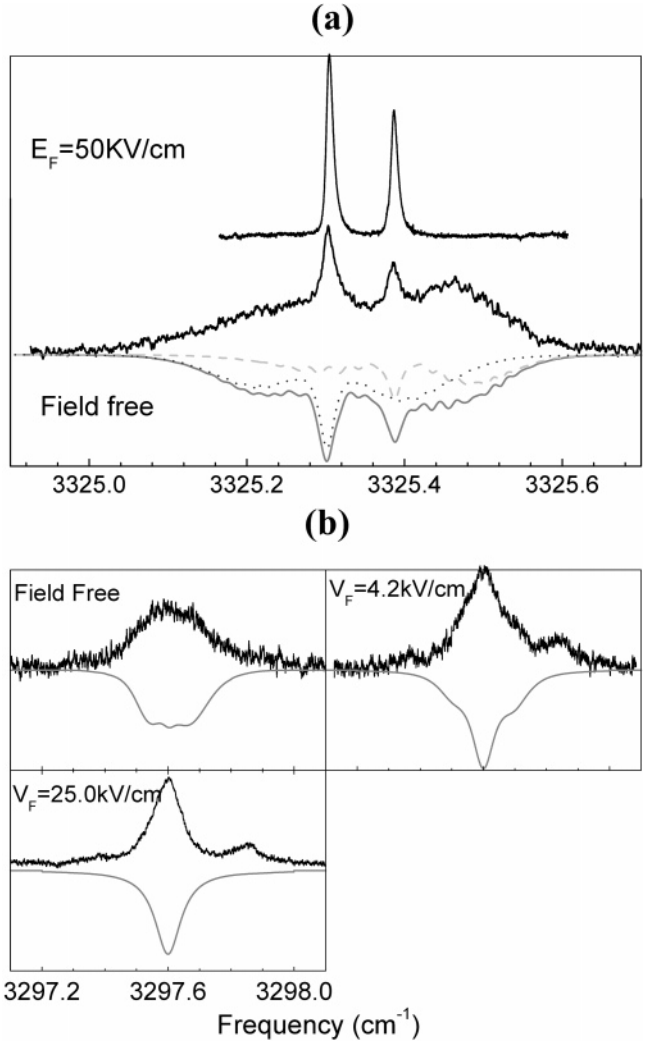

Figure 8. The field free and Stark spectra of HCCCN−Mg_2 for both the N-bonded (a) and H-bonded (b) isomers. The pendular spectrum provides an accurate determination of the vibrational band origins for two N-bonded isomers; so these are held fixed in the fit to the field free spectrum. The simulated spectra are again consistent with the ab initio structures **2(a)** and **2(b)** in Figure 2. The spectra in panel b are consistent with the H-bonded isomer and yield a dipole moment of approximately 4.9 D.

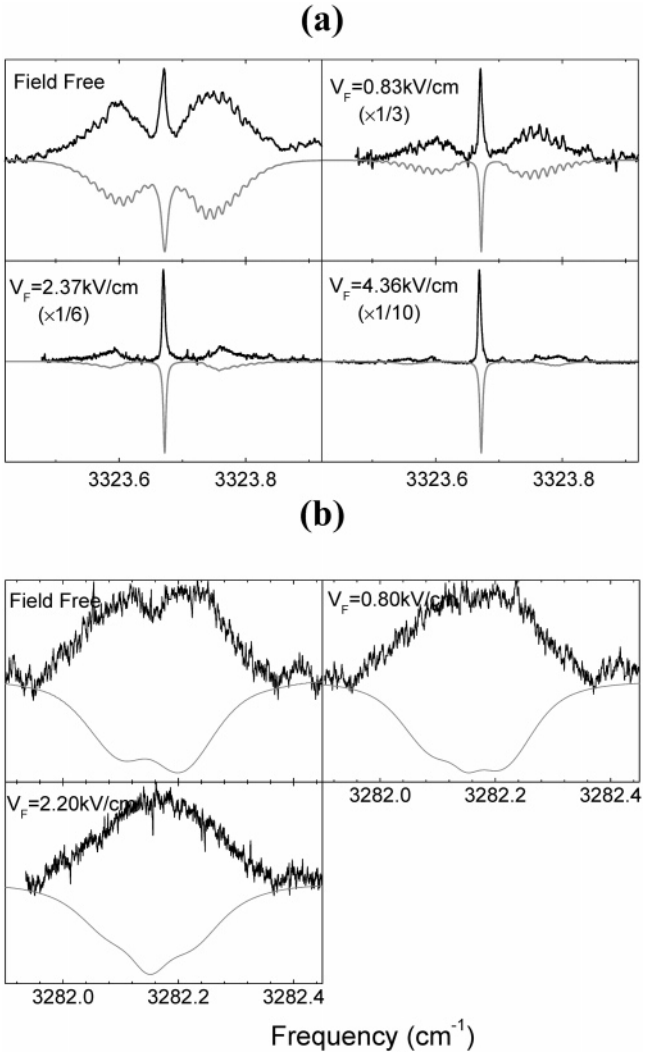

Figure 9. Field free and Stark spectra of N-bonded (a) and H-bonded (b) isomers of cyanoacetylene−Mg_3. The high symmetry (C_{3v}) of the nitrogen-bonded complex results in considerable rotational structure in the spectrum. The fits to the spectra give rotational constants that are consistent with the ab initio structure, when corrected for the effects of the helium. The dipole moments determined from the Stark spectra of these two isomers are 5.2 and 4.5 D for structures (3a) and (3b), respectively.

The ab initio calculations also predict the existence of a hydrogen-bonded isomer (see Table 2), with a calculated vibrational frequency shift of 28.3 cm^{-1}. As shown in Figure 8b, we observed a band at 3297.6 cm^{-1}, corresponding to an experimental vibrational frequency shift of 29.5 cm^{-1}. The oven temperature and pick-up cell pressure dependence of this band confirm that it was indeed associated with a (1,2) complex. The agreement between the ab initio and experimental frequency shifts leaves little doubt that this is the hydrogen-bonded Mg_2−HCCCN complex. The field free spectrum is more poorly resolved in this system, compared with that of Mg−HCCCN discussed above. Nevertheless, a fit to the overall contour is obtained with constants that are of reasonable magnitude, compared to the ab initio calculations, accounting for the effects of the helium (see Table 2). The electric field dependence of this vibrational band gave an estimated dipole moment of this complex of 4.9 ± 0.5 D, in excellent agreement with the ab initio value (4.89 D).

HCCCN−Mg_3. As noted in the ab initio section of this paper, the most stable structures for the Mg_3−HCCCN complex have the molecule lying along the 3-fold axis, with the magnesium cluster at either the nitrogen or hydrogen end. The N-bonded complex is clearly evident in the pendular spectrum in Figure 6b, labeled as (1,3). This peak grows in more slowly with increasing oven temperature, compared to the smaller magnesium complexes. Here again, the experimental vibrational frequency shift clearly indicates that the magnesium cluster is bonded to the nitrogen end of the cyanoacetylene. Indeed, the comparison between the experimental (3.417 cm^{-1}) and calculated (5.68 cm^{-1}) frequency shifts is quite reasonable, certainly compared to the much larger shifts associated with the hydrogen-bonded complex. As is now routine, the (1,3) assignment of this band is based upon the oven temperature and pick-up cell pressure dependence of the associated signals.

The zero-field spectrum of this (1,3) complex is shown in Figure 9a, along with several Stark spectra recorded at different electric fields. In this case, the zero-field spectrum is well resolved, owing to the high symmetry of the complex, and can be accurately fit to a symmetric top Hamiltonian. The rotational constants obtained from fitting the zero-field spectrum are summarized in Table 3. Note that the A rotational constant for

this complex is determined from the relative intensities of the P, Q, and R branches, which is possible given that the rotational temperature is known. Here again, the experimental values are a factor of approximately 3 smaller than those from ab initio theory. All of the Stark spectra presented in this paper were calculated by diagonalizing the full Hamiltonian matrix for a linear, symmetric, or asymmetric top molecule. The dipole moment obtained from the fits to the Stark spectra of HCCCN−Mg_3 shown in Figure 9a is 5.2 ± 0.2 D, in excellent agreement with the ab initio value of 5.08 D.

Searches for the hydrogen-bonded (1,3) complex revealed the spectra shown in Figure 9b. The experimental frequency shift is 44.94 cm^{-1}, in good agreement with the ab initio result (39.77 cm^{-1}). As we have come to expect, the broadening in the spectrum of this hydrogen-bonded complex is considerably greater than that for the nitrogen-bonded species, such that individual rotational transitions are not observed. As a result, the fits to these data are more qualitative and the corresponding molecular constants are less well determined (see Table 3). From the fits to the Stark spectra presented in Figure 9b we estimate the dipole moment of this complex to be ∼4.5 D, compared to the ab initio value of 4.72 D. The somewhat smaller dipole moment of this isomer results from the fact that the most polar part of the cyanoacetylene in the H-bonded complex is further from the magnesium atoms than in the N-bonded complex.

HCCCN−Mg_4. The bare Mg_4 complex has been the subject of considerable study and is well-known to have a regular tetrahedron structure, with considerably stronger interactions (0.30 eV/atom) (also reflected in the shorter bond lengths (3.045Å)) than the smaller clusters.[59,60] In previous studies of the N-bonded HCN−Mg_4 complex,[47] we found that the C−H stretch vibrational frequency shift was much larger than that for the smaller complexes. Comparisons with ab initio calculations revealed that there is a significant change in the nature of the bonding between the HCN and the magnesium cluster in going from $n = 3$ to $n = 4$. The structure of the corresponding nitrogen-bonded $n = 3$ complex was the same as discussed above for the HCCCN. For $n = 4$, the molecule prefers the "on-top" site, namely binding to a single magnesium atom in the Mg_4 cluster. A large increase in the dipole moment was also observed in going from $n = 3$ to $n = 4$, suggesting some degree of charge transfer between the molecule and the Mg_4 complex.

The ab initio calculations presented above suggest the same trend for the cyanoacetylene−Mg_n complexes. This behavior is clearly evident from the spectrum in Figure 5, with the band associated with HCCCN−Mg_4 appearing at 3318.68 cm^{-1}, corresponding to a frequency shift of 8.4 cm^{-1} from the HCCCN monomer. Once again, the peak labeled with $n = 4$ in Figure 5 was assigned by varying the Mg-oven temperature and the HCCCN pick-up cell pressure. The corresponding ab initio vibrational frequency shift for the nitrogen-bonded HCCCN−Mg_4 complex is 8.45 cm^{-1}. The zero-field spectrum of the (1,4) complex is shown in Figure 10a, along with the spectra recorded at three different electric fields. The high symmetry of this complex once again makes the rotational band rather well resolved, even though this is the largest complex studied thus far. The fitted spectra are also shown and the resulting molecular constants are summarized in Table 4. Here again, the rotational constants obtained from the fit are approximately a factor of 3 smaller than the ab initio values. Note the large experimental dipole moment that is obtained from these fits (9.3 D), consistent with that obtained from the ab initio calculations (9.99 D). In our previous study of the HCN−Mg_n complexes,[63] where a similarly large dipole was observed for $n = 4$, we presented ab initio calculations that suggested that this was due to charge transfer from the nitrogen lone pair to the magnesium cluster. As a result, we expect that the charge transfer will be highly dependent on the geometry of the complex, making the study of other isomers of fundamental interest.

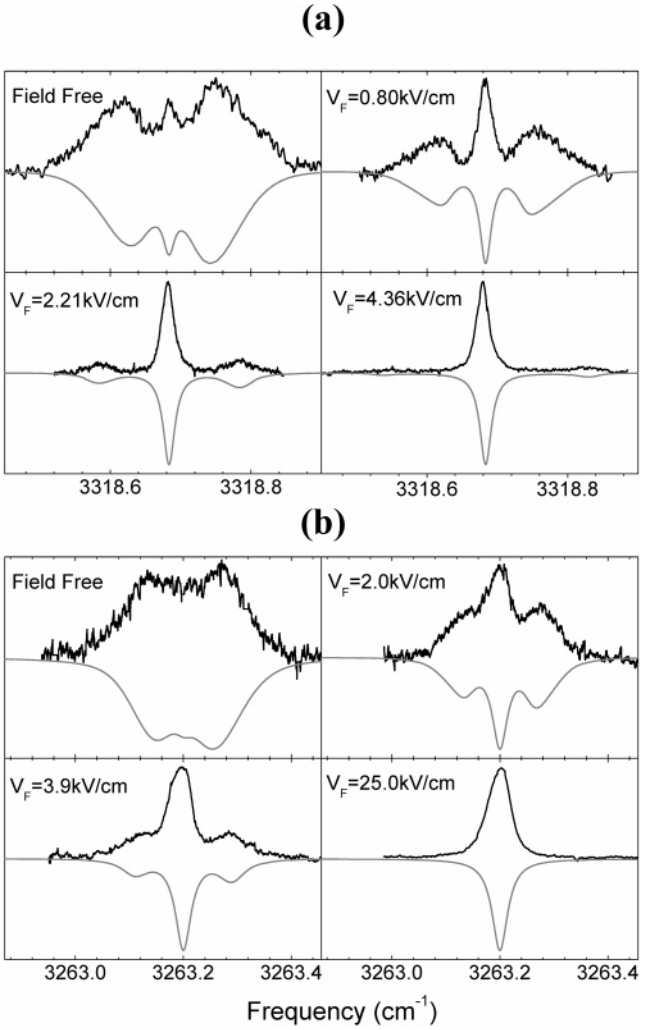

Figure 10. Field free and Stark spectra of N-bonded (a) and H-bonded (b) isomers of cyanoacetylene−Mg_4. The fits to the spectra give rotational constants that are consistent with the ab initio structure, when corrected for the effects of the helium. The dipole moments determined from the Stark spectra of these two isomers are 9.3 and 5.3 D for structures **4(a)** and **4(b)**, respectively.

Ab initio calculations suggest that the spectrum of the hydrogen-bonded isomer of Mg_4−HCCCN will be shifted by 65.55 cm^{-1} from the monomer. Searches in this and surrounding regions of the spectrum revealed the band shown in Figure 10b, with a frequency shift of 63.89 cm^{-1}. Although the reader could get the impression that there are bands everywhere and that we simply find them wherever they are predicated by the ab initio calculations, we note that many of the bands were actually found and assigned (based upon the oven temperature and pick-up cell pressure dependence of the corresponding signals) before the calculations were performed. As illustrated in the pendular spectrum shown in Figure 11, the bands assigned above are the only ones of significant intensity in this spectral region. Note that the maximum signals for both the N-bonded and H-bonded series in this spectrum occur for the $n = 3$ complex. Actually, the band associated with isomer **3(a)** is anomalously intense in this pendular spectrum owing to its relatively narrow width.

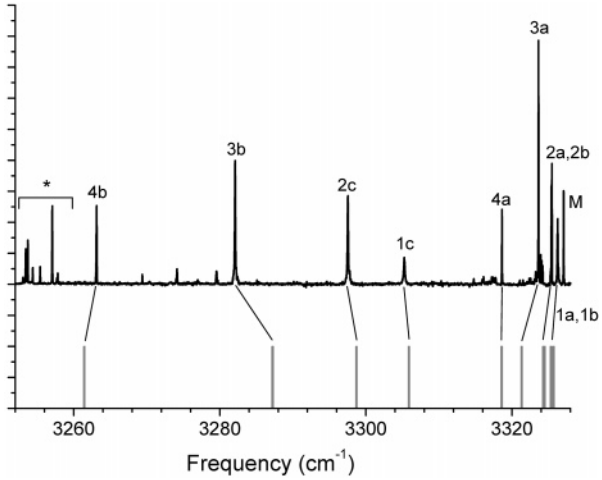

Figure 11. A survey scan of the pendular spectrum of the cyanoacetylene/magnesium clusters. The labels on the pendular peaks correspond to the structures given in Figures 1−4. The weak peaks and those marked with an asterisk are due to clusters with multiple cyanoacetylene molecules or contaminants from the background gases in the chamber.

Nevertheless, the intensities of these two series, assigned to the N-bonded and H-bonded complexes, illustrate further the assignments determined above. The minor peaks in the spectrum (including those marked with an asterisk) are associated with either complexes containing more than one cyanoacetylene molecule or background gases picked-up from the chamber.

The frequency shift of this hydrogen-bonded $n = 4$ complex is not unusually large, when compared to the smaller hydrogen-bonded species, implying that the anomalously large shift observed for the nitrogen-bonded complex is specific to the interaction with the nitrogen lone pair. This is also reflected in the dipole moment of the hydrogen-bonded complex, which was determined from the fit to the Stark spectra in Figure 10b (5.3 D), much smaller than for the nitrogen-bonded complex. A fit to the zero-field spectrum is also shown in Figure 10b, resulting in the constants summarized in Table 4.

Discussion

The extensive experimental and ab initio data presented above, for complexes between magnesium and cyanoacetylene, suggest that all of the minima on the corresponding potential energy surfaces are populated in these helium droplet experiments, providing us with a means of studying different portions of the PES. This is in contrast with what has been observed previously for clusters formed from polar molecules, such as HCN and HCCCN, where the growth in helium is dominated by long-range dipole−dipole interactions, resulting in the exclusive formation of linear chains.[43] Apparently the polar cyanoacetylene molecule approaches the nonpolar metal complexes with random orientation, resulting in the population of all of the local minima. Given this, it is interesting to consider what will happen when a molecule is added to the droplets first, followed by the metal atoms. In this case, we expect that the metal atoms will "land on" the molecule from random directions, becoming trapped in local minima that are remote from one another (in the present case, at opposite ends of the molecule, for example). This approach could be used to form even more exotic isomers, where the molecule is effectively coated by the metal atoms. Studies of this type are underway and will be the subject of future reports.

The vibrational frequency shifts measured as a function of cluster size and structure can provide important insights into

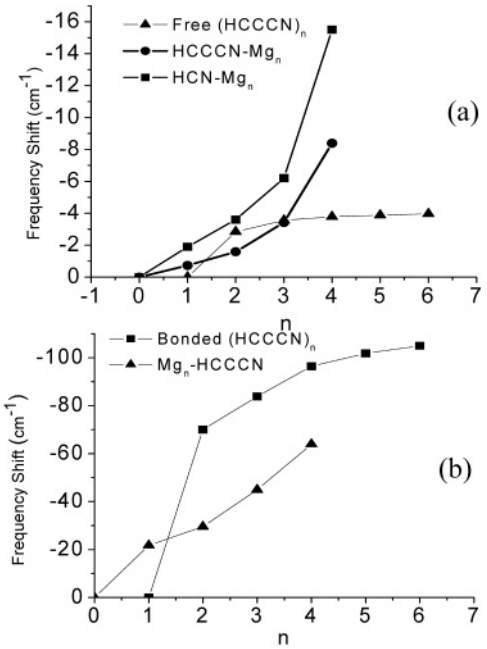

Figure 12. (a) A plot of the frequency shifts as a function of cluster size for the free C−H stretches of HCCCN−Mg_n, $(HCCCN)_n$, and HCN−Mg_n. (b) A plot of the frequency shifts for the H-bonded stretches of $(HCCCN)_n$ and Mg_n−HCCCN, Note that the large increase in the frequency shift observed in going from $n = 3$ to $n = 4$ for the nitrogen-bonded magnesium complexes is not seen for the hydrogen-bonded species. In addition, the frequency shifts for the free C−H stretch of HCCCN−Mg_n complexes are considerably smaller than the corresponding values for HCN−Mg_n.

the nature of the interactions in these systems. As summarized in Figure 12a, there is a qualitative difference in behavior for the linear $(HCCCN)_n$ clusters and the magnesium clusters considered here. In the former case, the frequency shifts for the terminal or "free" C−H stretch (solid triangles in Figure 12a) smoothly saturate with increasing cluster size, at a rather small value (approximately 4 cm^{-1}). This is easily understood given that the "free" C−H stretch is rather well localized at the terminus of the chain, so that the addition of molecules at the other end becomes less important with increasing cluster size. The situation is clearly different for the "free" C−H stretch of the cyanoacetylene−Mg_n complexes (solid circles in Figure 12a). As discussed above, the shift for the $n = 4$ complex is substantially larger than that of the smaller complexes, suggesting that the interactions are highly nonadditive. Note from Figure 12a that the same behavior is seen in HCN−Mg_n, although the absolute magnitudes of the shifts are larger in this case. This makes sense given the relative proximity of the C−H stretch to the binding site for these two molecules. As noted above, the large frequency shifts observed for the $n = 4$ magnesium complexes are consistent with the relatively strong bonding in these complexes.

The frequency shifts associated with the hydrogen-bonded C−H stretches of the linear cyanoacetylene chains also shift smoothly with chain length, as shown in Figure 12b, once again converging to a limiting value. In this case, the shifts are much larger (>100 cm^{-1}) than for the "free" C−H stretches, owing to the much stronger coupling between the intramolecular vibrations and the hydrogen bond. Similarly, the shifts for the hydrogen-bonded magnesium clusters are much larger than those for the nitrogen-bonded complexes. Nevertheless, as shown in Figure 12b, the frequency shifts increase almost linearly with increasing magnesium cluster size, showing nothing special

TABLE 5: Comparisons of Bond Distances (Å) in Free Magnesium Clusters, HCN−Mg_n, and HCCCN−Mg_n

	Mg_n[a]	HCN−Mg_n[b]		HCCCN−Mg_n		
n	R_{Mg-Mg} (Å)	R_{N-Mg} (Å)	R_{Mg-Mg} (Å)	isomers	R_{N-Mg} (Å)	R_{Mg-Mg} (Å)
1		3.778		**1a**	3.588	
				1b	4.368	
				1c	3.598[c]	
2	4.094	3.762	3.917	**2a**	3.553	3.887
				2b	3.399	3.863
				2c	3.541[c]	3.952
3	3.369	3.416	3.261	**3a**	3.111	3.207
				3b	3.264[c]	3.376
4	3.045	2.396	3.038, 2.986	**4a**	2.350	3.039, 2.985
		3.604[c]	3.032, 3.045	**4c**	3.580[c]	3.044, 3.037

[a] Calculated at the MP2/6-311++G(3df,3pd) level with Gaussian98. [b] References 46 and 47. [c] R_{H-Mg} in the H-bonded isomers.

occurring at $n = 4$. Similarly, the dipole moments for these hydrogen-bonded complexes show nothing unusual for the $n = 4$ complex. This is consistent with the charge transfer mechanism observed in the nitrogen-bonded complex no longer being important for this isomer, as would be expected from geometrical considerations. The interactions involving the magnesium tetramer are clearly not indiscriminately large, but rather strongly dependent on the orientation of the molecule relative to the cluster. This is consistent with the idea that charge transfer between the lone pair on the nitrogen of cyanoacetylene plays an important role in determining the special character of the nitrogen-bonded $n = 4$ isomer. Indeed, the on-top structure of this isomer is consistent with charge donation from the nitrogen lone pair to the lowest unoccupied molecular orbital (LUMO) of the Mg_4, a point that is discussed elsewhere for other adsorbate−metal systems.[47] It is also interesting to note that the HOMO of Mg_4 places considerable electron density on the 3-fold site,[47] accounting for the fact that the electropositive hydrogen atoms of cyanoacetylene prefer to bind at this location. Similar arguments, based upon the HOMOs and LUMOs, work equally well in explaining the structures observed for HCCCN−Mg_3.

The ab initio bond lengths for the various complexes discussed here, including those of HCN and the bare magnesium clusters, are summarized in Table 5. These results show that there are rather significant changes in the values of R_{N-Mg} and R_{Mg-Mg} with cluster size. It is noteworthy that R_{N-Mg} for the nitrogen-bonded $n = 4$ complex is particularly short, namely 2.35 Å, compared to that of the binary complex, namely 3.588 Å. Such a large change in bond length over a rather small cluster size range is unusual (i.e. not seen in van der Waals systems), providing further evidence that the interactions in these systems are highly nonadditive.

All of the complexes considered here have been treated as if they were rigid. We have not discussed the possibility that they undergo wide amplitude motions, which might include tunneling through the rather low barriers between the local minima on the PES. The main reason for this apparent oversight is simply that the spectra observed here do not provide information on these motions. All of the spectra reported here could be adequately fit by rigid rotor energy level expressions (in some cases modified by centrifugal distortion constants). All indications are that the barriers between the local minima in these systems are sufficiently high to prevent interconversion at the droplet temperature, even though we cannot completely rule out this possibility.

Conclusions

We have presented a detailed experimental and ab initio study of the complexes of cyanoacetylene with magnesium clusters, formed in the liquid helium droplets. Multiple isomers have been observed for the various cluster sizes. The observation of these different isomers confirms that the rapid cooling provided by the helium, during the cluster formation process, is sufficient to trap the system in metastable structures. This is despite the fact that, according to ab initio calculations, the barriers between some of these are quite low. The agreement between experiment and theory is remarkably good for all of the systems studied here, illustrating how the two can be used to obtain deeper insights into the nature of the interactions in these systems. In fact, magnesium was chosen as a starting point in our study of metal complexes because of the relative ease with which it can be treated by ab initio theory, in comparison to the transition metals.

The interactions in these systems have been shown to be highly nonadditive and highly structurally specific. Theory and experiment agree that the interactions in the nitrogen-bonded $n = 4$ complex are anomalously strong, as is the associated electric dipole moment. Indications are that the latter is due to charge transfer from the lone pair on the nitrogen molecule to the LUMO of the magnesium tetramer. The experimental method used here is quite general and plans are underway to study the analogous transition metal complexes. In addition, further work is needed on larger magnesium complexes, with the goal of studying systems near the insulator-to-metal transition,[64] in order to provide insights into the associated changes in the adsorbate binding.

Acknowledgment. This work was supported by the National Science Foundation (CHE-99-87740) and the Air Force Office of Scientific Research.

References and Notes

(1) Ballore P.; Andreoni, W. *Metal Clusters*; John Wiley & Sons: West Sussex, England, 1999; pp 71−136.
(2) Bauschlicher, C. W.; Partridge, H. *Chem. Phys. Lett.* **1999**, *300*, 364−368.
(3) Braunstein P.; Rose, J. *Metal Clusters in Chemistry*; Wiley-VCH: New York, 1998; Chapter 2.2, pp 616−677.
(4) Cheng, H. P.; Ellis, D. E. *J. Chem. Phys.* **1991**, *94*, 3735−3747.
(5) Edwards P. P.; Johnston, R. L.; Rao, C. N. R. *Metal Clusters in Chemistry*; Wiley-VCH: New York, 1998; Chapter 4.8, pp 1454−1481.
(6) Fantucci, P.; Koutecky, J.; Pacchioni, G. *J. Chem. Phys.* **1984**, *80*, 325−328.
(7) Heinz K.; Broer, M. *Advance in Metal and Semiconductor Clusters*; JA1 Press Inc.: Greenwich, CT, 1993; Chapter 2, pp 37−82.
(8) Heiz, U.; Vanolli, F.; Sanchez, A.; Schneider, W. D. *J. Am. Chem. Soc.* **1998**, *120*, 9668−9671.
(9) Jos de Jongh L. *Metal Clusters in Chemistry*; Wiley-VCH: New York, 1998; Chapter 4.7, pp 1434−1453.
(10) Kaplan, I. G. *Int. J. Quantum Chem.* **1999**, *74*, 241−247.
(11) Klabunde, K. J.; Whetten, A. *J. Am. Chem. Soc.* **1986**, *108*, 6529−6534.
(12) Knickelbein, M. B. *Annu. Rev. Phys. Chem.* **1999**, *50*, 79−115.
(13) Lindsay, D. M.; Chu, L.; Wang, Y.; George, T. F. *J. Chem. Phys.* **1987**, *87*, 1685−1689.
(14) Mcintyre, B. J.; Salmeron, M.; Somorjai, G. A. *Science* **1994**, *265*, 1415−1418.
(15) Pacchioni G.; Kruger, S.; Rosch, N. *Metal Clusters in Chemistry*; Wiley-VCH: New York, 1998; Chapter 4.6, pp 1393−1433.
(16) Puddephatt R. J. *Metal Clusters in Chemistry*; Wiley-VCH: New York, 1998; Chapter 2.1, pp 605−615.
(17) Schmid G. *Metal Clusters in Chemistry*; Wiley-VCH: New York, 1998; Chapter 4.3, pp. 1325−1341.
(18) Ulvenlund S.; Bengtsson-Kloo, L. *Metal Clusters in Chemistry*; Wiley-VCH: New York, 1998; Chapter 1.29, pp 561−602.
(19) Uppenbrink, J.; Wales, D. J. *J. Chem. Phys.* **1992**, *96*, 8520−8534.
(20) Uppenbrink, J.; Wales, D. J. *J. Chem. Phys.* **1993**, *98*, 5720−5733.

(21) Wang, L. S.; Cheng, H. S.; Fan, J. *J. Chem. Phys.* **1995**, *102*, 9480−9493.
(22) Wang L. S.; Wu, H. *Advance in Metal and Semiconductor Clusters*; JA1 Press: Greenwich, CT, 21998; pp 299−343.
(23) Smalley, R. E. *Springer Ser. Opt. Sci.* **1985**, *49*, 317−319.
(24) Jortner J. *Physics and Chemistry of Finite Systems: From Clusters to Crystals*; 1992; Vol. I, pp 1−17.
(25) Delaly, P.; Ballone, P.; Buttet, J. *Phys. Rev. B* **1992**, *45*, 3838−3841.
(26) Diederich, T.; Doppner, T.; Braune, J.; Tiggesbaumker, J.; Meiwes-Broer, K. H. *Phys. Rev. Lett.* **2001**, *86*, 4807−4810.
(27) Histed, M.; Howard, J. A.; Jones, R.; Tomietto, M. *J. Chem. Soc., Perkin Trans. 2* **1993**, 267−272.
(28) Jasien, P. G.; Dykstra, C. E. *J. Am. Chem. Soc.* **1985**, *107*, 1891−1895.
(29) Knickelbein, M. B. *J. Chem. Phys.* **2002**, *116*, 9703−9711.
(30) Koretsky, G. M.; Knickelbein, M. B. *J. Chem. Phys.* **1997**, *107*, 10555−10566.
(31) Knickelbein, M. B.; Menezes, W. J. C. *Chem. Phys. Lett.* **1991**, *184*, 433−438.
(32) Sanchez, A.; Abbet, S.; Heiz, U.; Schneider, W. D.; Hakkinen, H.; Barnett, R. N.; Landman, U. *J. Phys. Chem. A* **1999**, *103*, 9573−9578.
(33) Cunningham, D. A. H.; Vogel, W.; Kageyama, H.; Tsubota, S.; Haruta, M. *J. Catal.* **1998**, *177*, 1−10.
(34) Rienstra-Kiracofe, J. C.; Tschumper, G. S.; Schaefer, H. F.; Nandi, S.; Ellison, G. B. *Chem. Rev.* **2002**, *102*, 231−282.
(35) Felix, C.; Sieber, C.; Harbich, W.; Buttet, J.; Rabin, I.; Schulze, W.; Ertl, G. *Phys. Rev. Lett.* **2001**, *86*, 2992−2995.
(36) Rosendo-Francisco, P.; Lupulescu, C.; Baptist, B.; Vajda, S. *J. Chin. Chem. Soc.* **2000**, *47*, 705−708.
(37) Woste, L. *Opt. Appl.* **1999**, *29*, 543-+.
(38) von Busch, H.; Demtroder, W.; Dev, V.; Eckel, H. A.; Grosskloss, R.; Keil, M.; Kramer, H. G.; Platz, T.; Wenz, H. *Phys. Scr.* **1999**, *59*, 147−151.
(39) Riley S. J.; Parks, E. K. *Physics and Chemistry of Finite Systems: From Clusters to Crystals*; 1992; Vol. I, pp 19−28.
(40) Callegari, C.; Lehmann, K. K.; Schmied, R.; Scoles, G. *J. Chem. Phys.* **2001**, *115*, 10090−10110.
(41) Hartmann, M.; Miller, R. E.; Toennies, J. P.; Vilesov, A. F. *Science* **1996**, *272*, 1631−1634.
(42) Lehmann, K. K.; Scoles, G. *Science* **1998**, *279*, 2065−2066.
(43) Nauta, K.; Miller, R. E. *Science* **1999**, *283*, 1895−1897.
(44) Nauta, K.; Miller, R. E. *Science* **2000**, *287*, 293−295.
(45) Nauta, K.; Moore, D. T.; Stiles, P. L.; Miller, R. E. *Science* **2001**, *292*, 481−484.
(46) Stiles, P. L.; Moore, D. T.; Miller, R. E. *J. Chem. Phys.* **2003**, *118*, 7873−7881.
(47) Stiles, P. L., Moore, D. T.; Miller, R. E. *J. Chem. Phys.* Submitted for publication.
(48) Nauta, K.; Moore, D. T.; Miller, R. E. *Faraday Discuss.* **1999**, *113*, 261−278.
(49) Nauta, K.; Miller, R. E. *J. Chem. Phys.* **1999**, *111*, 3426−3433.
(50) Gough, T. E.; Mengel, M.; Rowntree, P. A.; Scoles, G. *J. Chem. Phys.* **1985**, *83*, 4958−4961.
(51) Gough, T. E.; Miller, R. E.; Scoles, G. *Appl. Phys. Lett.* **1977**, *30*, 338−340.
(52) Jucks, K. W.; Miller, R. E. *J. Chem. Phys.* **1987**, *87*, 5629−5633.
(53) Stiles, P. L.; Nauta, K.; Miller, R. E. *Phys. Rev. Lett.* **2003**, *90*, 135301.
(54) MOLPRO 2002. Birmingham, UK.
(55) Boys, S. F.; Bernardi, F. *Mol. Phys.* **1970**, *19(4)*, 553−566.
(56) Frisch, M. J.; Trucks, G. W.; Schlegel, H. B.; Scuseria, G. E.; Robb, M. A.; Cheeseman, J. R.; Zakrzewski, V. G.; Montgomery, J. A., Jr.; Stratmann, R. E.; Burant, J. C.; Dapprich, S.; Millam, J. M.; Daniels, A. D.; Kudin, K. N.; Strain, M. C.; Farkas, O.; Tomasi, J.; Barone, V.; Cossi, M.; Cammi, R.; Mennucci, B.; Pomelli, C.; Adamo, C.; Clifford, S.; Ochterski, J.; Petersson, G. A.; Ayala, P. Y.; Cui, Q.; Morokuma, K.; Malick, D. K.; Rabuck, A. D.; Raghavachari, K.; Foresman, J. B.; Cioslowski, J.; Ortiz, J. V.; Stefanov, B. B.; Liu, G.; Liashenko, A.; Piskorz, P.; Komaromi, I.; Gomperts, R.; Martin, R. L.; Fox, D. J.; Keith, T.; Al-Laham, M. A.; Peng, C. Y.; Nanayakkara, A.; Gonzalez, C.; Challacombe, M.; Gill, P. M. W.; Johnson, B. G.; Chen, W.; Wong, M. W.; Andres, J. L.; Head-Gordon, M.; Replogle, E. S.; Pople, J. A. *Gaussian 98*; Gaussian, Inc.: Pittsburgh, PA, 1998.
(57) Moore, D. T.; Miller, R. E. Unpublished work
(58) Douberly, G. E.; Miller, R. E. *J. Phys. Chem. A* **2003**, *107*, 4500−4507.
(59) Kohn, A.; Weigend, F.; Ahlrichs, R. *Phys. Chem. Chem. Phys.* **2001**, *3*, 711−719.
(60) Lee, T. J.; Rendell, A. P.; Taylor, P. R. *J. Chem. Phys.* **1990**, *93*, 6636−6641.
(61) *CRC Handbook of Chemistry and Physics*, 71st ed.; Chemical Rubber Co.: Boca Raton, FL, 1990.
(62) Nauta, K.; Miller, R. E. *J. Chem. Phys.* **2001**, *115*, 10138−10145.
(63) Bittererova, M.; Brinck, T.; Ostmark, H. *J. Phys. Chem.* **2000**, *104*, 11999−12005.
(64) Thomas, O. C.; Zheng, W.; Xu, S.; Bowen, K. H. *Phys. Rev. Lett.* **2002**, *89*, 213403.